JACS
JOURNAL OF THE AMERICAN CHEMICAL SOCIETY

ARTICLE

pubs.acs.org/JACS

Mechanism of Formation of the Internal Aldimine in Pyridoxal 5′-Phosphate-Dependent Enzymes

Eduardo F. Oliveira, Nuno M. F. S. A. Cerqueira, Pedro A. Fernandes, and Maria J. Ramos*

REQUIMTE, Faculdade de Ciências, Universidade do Porto, Rua Campo Alegre 687, 4169-007 Porto, Portugal

Supporting Information

ABSTRACT: In this paper we studied the mechanism of formation of the internal aldimine, a common intermediate to most pyridoxal 5′-phosphate (PLP)-dependent enzymes. A large model based on the crystal structure from the human ornithine decarboxylase (ODC) enzyme was constructed and in total accounts for 504 atoms. The reaction mechanism was investigated using the ONIOM methodology (B3LYP/6-31G(d)//AM1), and the final energies were calculated with the M06/6-311++G(2d,2p)//B3LYP/6-31G(d) level of theory. It was demonstrated that the reaction is accomplished in three sequential steps: (i) the nucleophilic attack of Lysine69 to PLP, (ii) the carbinolamine formation, and (iii) a final dehydration step. For the carbinolamine formation, several mechanistic hypotheses were explored, and the preferred pathway assigns a key role for the conserved active site Cys360. The overall reaction is exergonic in −9.1 kcal/mol, and the rate-limiting step is the dehydration step (E_a = 13.5 kcal/mol). For the first time, we provide an atomistic portrait of this mechanism in an enzymatic environment. Moreover, we were able to assign a novel role to Cys360 in the ODC reaction mechanism that was never proposed.

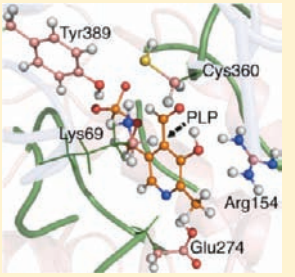

1. INTRODUCTION

Pyridoxal 5′-phosphate (PLP), commonly known as vitamin B6, is a cofactor employed by many enzymes to assist in the catalysis of many chemical reactions. It is estimated that PLP is required by more than 4% of all the enzymes. These enzymes play a central role in numerous metabolic pathways involving amino acids and catalyze a wide variety of chemical reactions, including transaminations, racemizations, aldol cleavages, α-decarboxylations, β- and γ-eliminations, and replacement reactions[1,2] (Scheme 1).

The key role of most of these enzymes in many fundamental biological pathways makes them appealing targets for several diseases and conditions. There are already promising attempts to treat epilepsy through the inhibition of γ-aminobutyric acid aminotransferase or to develop antibacterial agents that inhibit alanine racemase. The PLP-dependent enzyme ornithine decarboxylase (ODC) is the target of the suicide inhibitor α-difluoromethylornithine (α-DFMO) used to stop replication and growth of *Trypanosoma brucei*, the causative agent of African sleeping sickness. More recently, this enzyme aroused interest as a potential target against cancer. All these factors make the mechanism of these enzymes an active area of research that has witnessed a surge of interest in recent years.

The majority of PLP-dependent enzymes require the initial formation of an internal aldimine in which PLP becomes bonded to a highly conserved active site lysine residue, forming a Schiff base (Scheme 1). Only in this form do these enzymes become active. Subsequently, the PLP−enzyme complex reacts with the substrate, the bond with the active site lysine is broken, and a new Schiff base is formed with PLP attached to the amino substrate (commonly referred as the transimination reaction). The specific reaction that follows depends on the enzyme and on the type of substrate. In any case PLP acts as a key catalyst.[3,4]

In the past 30 years much attention has been centered on the transimination reaction because it is common to the majority of the PLP-dependent enzymes. However, the previous step of the catalytic cycle, which involves the formation of a Schiff base between the PLP and an active site lysine, has been disregarded. This step is also common to all of these enzymes, and the binding of the cofactor and its correct orientation in the active site depend on it. This will be the subject of this paper.

The formation of the Schiff base between PLP and the active site lysine results in a stable enzyme−PLP complex, generally called the internal aldimine. This reaction involves the nucleophilic attack of the ε-amine group from a lysine side chain (generally Lys69) to the aldehyde group of PLP. In spite of looking apparently simple, this reaction is complex and involves the formation of several intermediate species and the release of one water molecule. One of these intermediates is a carbinolamine-like coumpound, and its presence has already been supported by experimental evidence.[5] Several studies suggest that the rate-limiting step of this reaction is the dehydration step.[5−8] More recently, Salvà et al. performed density functional theory (DFT) calculations to study the formation of the internal aldimine using a model reaction containing 3-hydroxy-4′-pyridinealdehyde and methylamine.[9] Their results also suggest that the dehydration is the rate-determining step of this reaction. In spite of these results, there is a lack of knowledge regarding this mechanism in enzymatic environments.[10] In addition, several

Received: May 8, 2011
Published: August 21, 2011

Scheme 1. Schematic Representation of the Currently Accepted Mechanism for the Formation of the Internal Aldimine in PLP-Dependent Enzymes

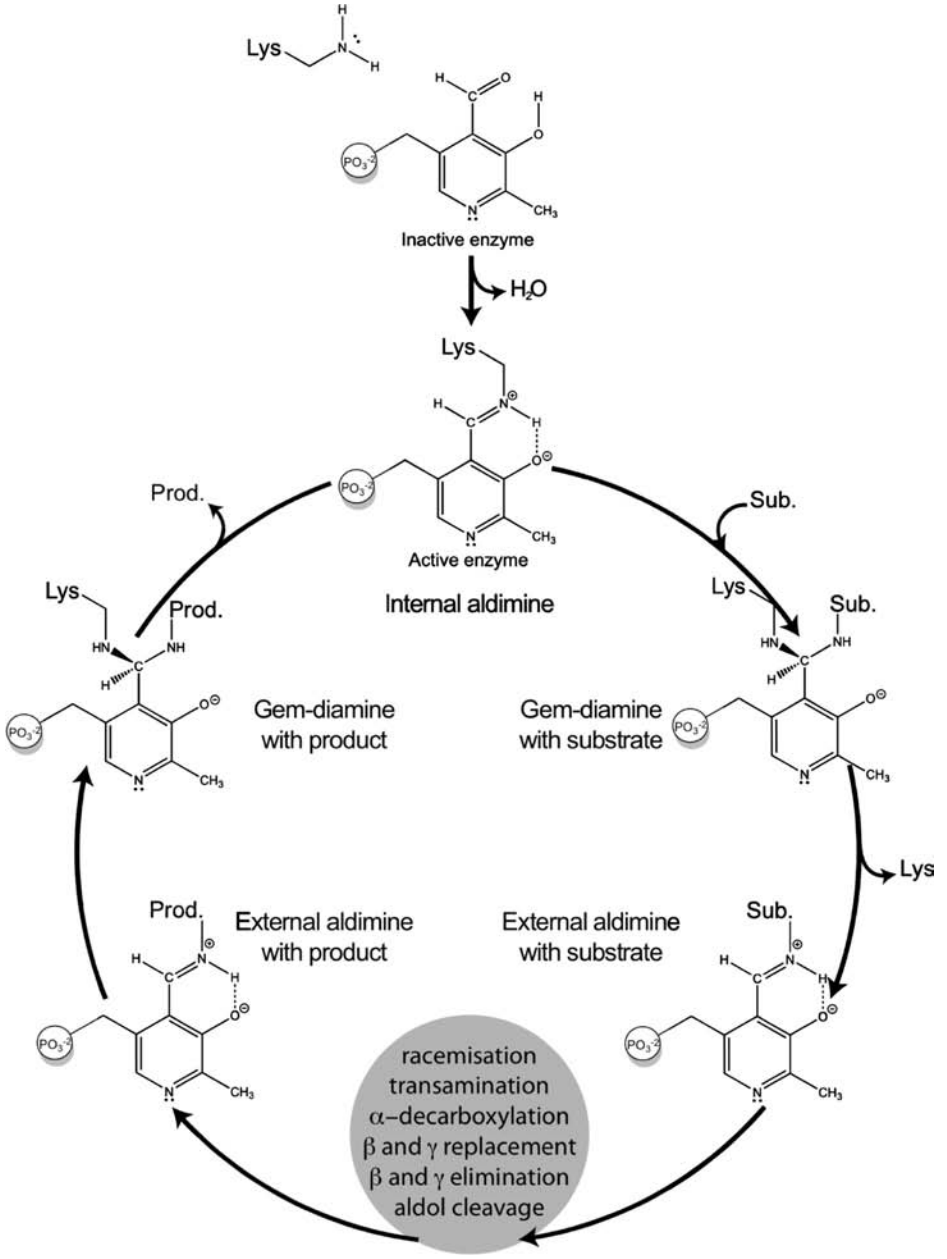

pieces of experimental evidence require further research, for instance, the involvement of the conserved Cys360 or the water molecule in the course of the reaction.

In this investigation, we study the mechanism of formation of the internal aldimine in PLP-dependent enzymes. This is a crucial step in the activation of these enzymes that has become a major milestone in this field to understand how these enzymes work. To attain this milestone, we will resort to computational methods that have been widely used in the past two decades to elucidate the chemical mechanism of many enzymatic reactions.[11−15] To study this reaction in particular, we have undertaken high-level theoretical calculations using an ONIOM (M06/6-311++G(2d,p2p):B3LYP/6-31G(d)//ONIOM(B3LYP/6-31G(d):AM1) scheme on a model of the human ODC enzyme. In this work we present the description of all the intermediates and transition-state structures along the reaction pathway that leads to the formation of the internal aldimine.

2. METHODS

2.1. Model. The model used in this work was based on the crystal structure of the human ODC (resolution 1.9 Å) determined by Dufe et al.[16] The active form is a homodimer. The active site is located at the interface between both subunits, close to a cavity formed by the loops from both monomers. The full system would include 14 000 atoms, but we choose to reduce its size to improve the efficiency of the calculations. Therefore, the model used here contains only PLP and a portion of each monomer, i.e., chains Ala67−Cys70, Phe87−Ala90, Leu153−Ile155,

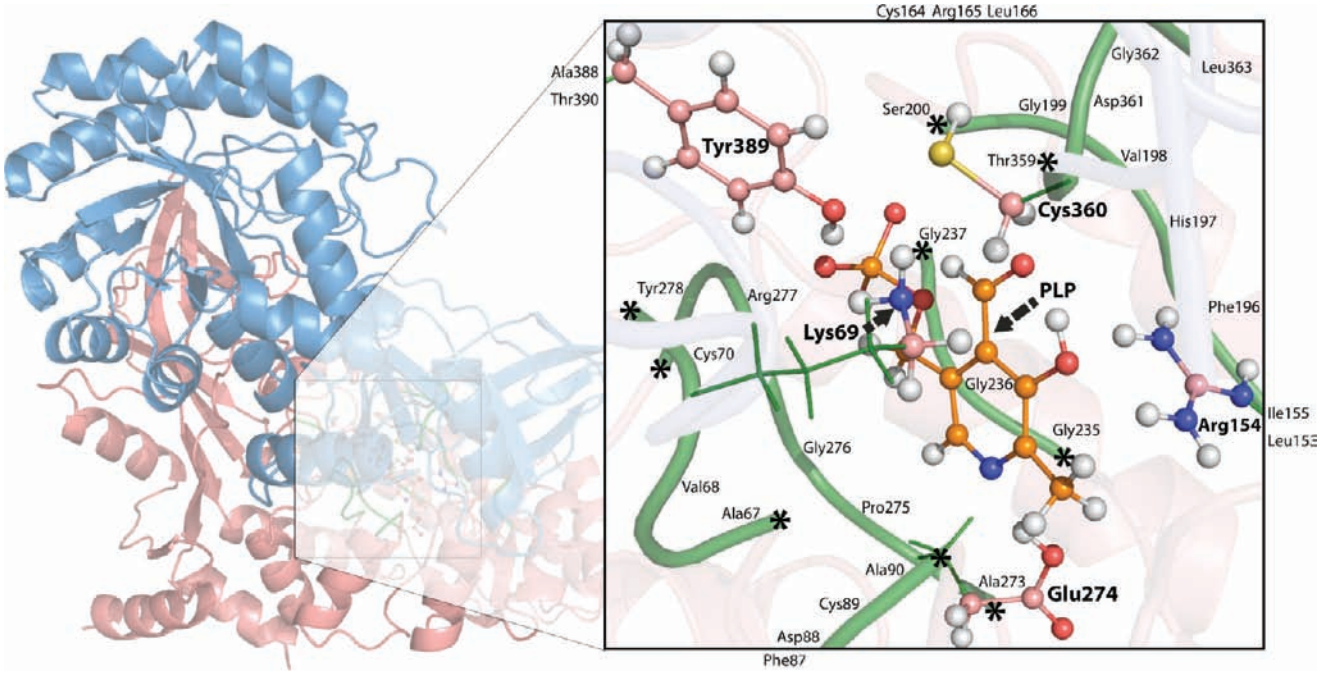

Figure 1. (Left) ODC homodimer (PDB ID 2OO0). Monomer A is colored red, and monomer 2 is colored blue. (Right) QM/QM model. The high-level layer is colored by element type and depicted in ball and stick format (66 atoms). The low-level layer is represented in cartoons and colored in green (504 atoms). The frozen atoms are marked with an asterisk.

Cys164−Leu166, Phe196−Ser200, Gly235−Gly237, Ala273−Tyr278, and Ala388−Thr390 from monomer A and chain Thr359−Leu363 from monomer B (Figure 1).

Hydrogen atoms were added to the model using the software Accelrys Discovery Studio.[17] Conventional protonation states for all amino acids at pH 7.5 were adopted, except for Lys69, which was left unprotonated, a condition that is required for the formation of the internal aldimine. The carboxylate and the amino groups of the terminal amino acids of each chain of the model were protonated. The final model accounts for a total of 504 atoms.

Subsequently, the geometry of the model was optimized at the QM/QM level. To keep the optimized structures close to the X-ray structure, the Cα coordinates of the terminal amino acids of each chain were frozen, as depicted in Figure 1.

2.2. Methods. As the system is very large, and geometry optimizations are very time-consuming, we have resorted to the ONIOM methodology to deal with the system.[18,19] This method allows to the system to be handled in several regions, each one studied with a different theoretical level. The accuracy of the method is dependent on the chosen regions and the theoretical level used in each of them. According to the ONIOM methodology, we have chosen a smaller cut of our 504-atom model to be treated with a higher theoretical level, designated the high-level layer. The high-level layer included all atoms from PLP plus part of the side chains of the residues that are directly involved in the reaction, namely, Lys69, Glu274, Arg154, Tyr389, and Cys360. This layer accounted for a total of 66 atoms. The low-level layer contained all the atoms of the model. The atoms described at the low level of theory did not undergo significant geometric changes during the reaction, but were still important to account for the correct orientation of the active site residues and for the medium/long-range interactions between the enzyme and the substrate. For bonds spanning between the two regions, we used hydrogen atoms as link atoms.

The geometry of the high-level layer was optimized with the higher theoretical level (DFT level). The B3LYP functional was chosen, since it is known to give very good results for organic molecules.[20] The 6-31G(d) basis set was employed, as implemented in Gaussian 09.[21] The inclusion of diffusion functions in the basis set for geometry optimizations was investigated previously.[22] The conclusion was that the corrections to the geometry were very small, and corrections in energy differences (such as energy barriers or energies of reaction) were negligible, upon the calculation of single-point energies with a more complete basis set. Therefore, it seems inadequate from a computational point of view to include diffuse functions in geometry optimizations, considering the inherent increase in computing time that they would cause. The low-level layer was treated with the semiempirical method AM1.[23]

The model, with the above-mentioned constraints, was fully optimized with the Gaussian 09 standard parameters. The final optimized geometry was superimposed with several ODC crystallographic structures, and no relevant geometry divergences were detected. Subsequently, several hypotheses for the reaction mechanism were explored through linear transit scans along the reaction coordinates implicated in the formation of the internal aldimine. From the electronic energy profile of each mechanism, two minima connected by a transition state were identifiable. The region on the potential energy surfaces closer to the maximum was further rescanned at narrower distance intervals (0.01 or 0.005 Å). The final energies of the minima and transition-state structures were additionally characterized by single-point energy determinations at the M06/6-311++G(2d,2p) level[24−26] in the high layer and the B3LYP/6-31G(d) level in the low layer. The atomic spin-density distributions were calculated at the B3LYP/6-31G(d) level employing a Merz−Singh−Kollman population analysis scheme.[27,28]

To estimate the error in the activation energies introduced by the constrained optimization of the transition states, we freely optimized the transition-state structure of the first step of the mechanism, starting from the higher energy structure in the linear transit scan. The calculation was extremely time-consuming (in particular the Hessian calculation) due to the very large size of the system. At the very end we confirmed its saddle point nature by analyzing the vibrational frequencies. The highest imaginary frequency (101i cm^{-1}) is dominated by a stretching vibration involving the bonds that are formed/broken in the reaction. The

Scheme 2. Proposed Intermediates for the Studied Reaction, Schiff Base Formation between PLP and Lys69

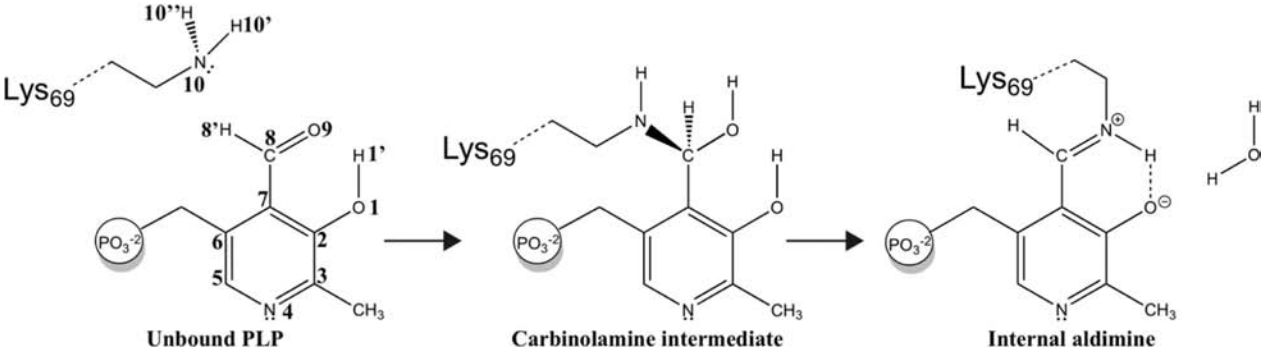

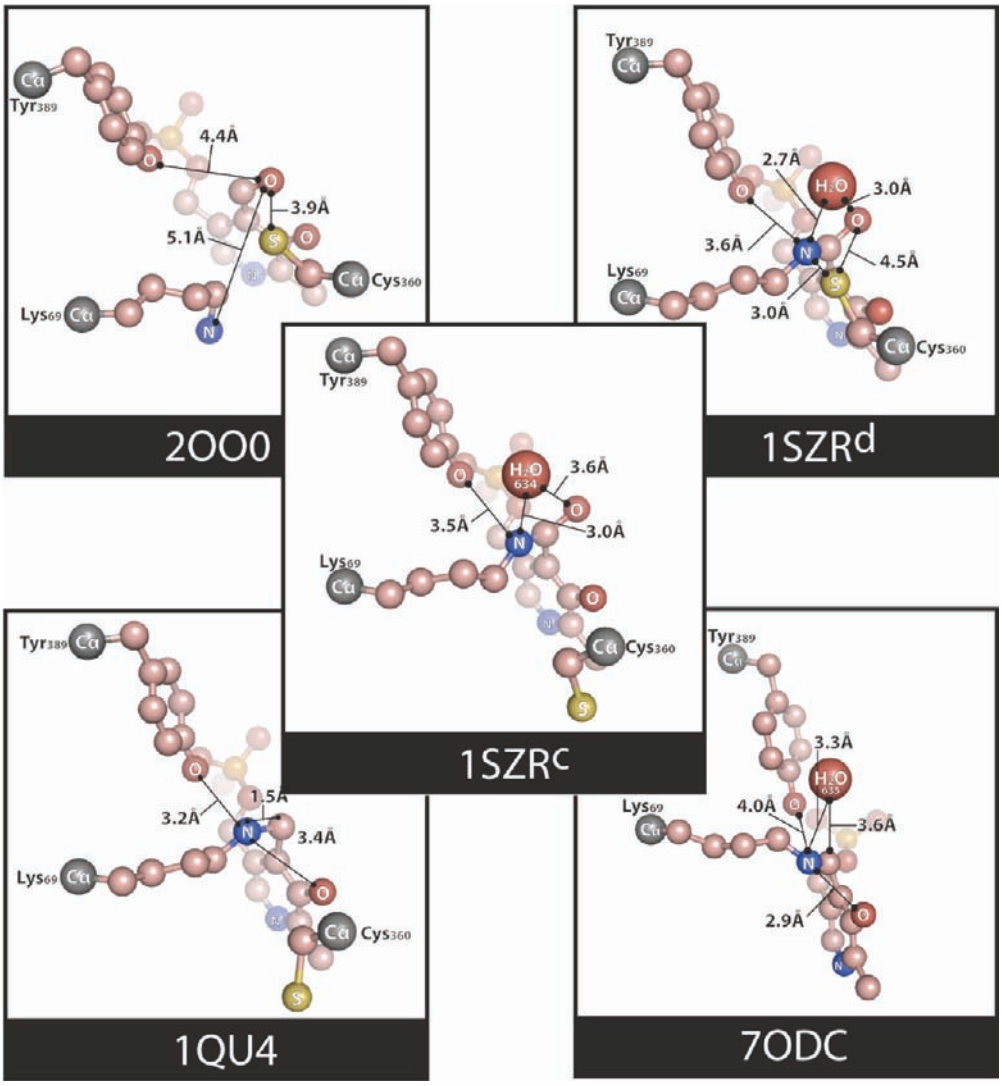

Figure 2. PDB structures of ODC that resemble several intermediates that might be involved in the formation of the internal aldimine.

activation energy calculated with this transition state was extremely close to the one derived from the linear transit scan (difference of 0.5 kcal/mol). In addition, there were no significant differences in the structures (rms = 0.02 Å). Taking this result into account, we decided to extract the transition-state structures of the remaining steps from the highest energy points of the correspondent linear transit scans.

3. RESULTS AND DISCUSSION

As the PLP enzymes have been extensively studied by X-ray crystallography over the past decade, there is a large source of information in the Protein Data Bank containing several inter mediate complexes that are involved in the formation of the

internal aldimine. In this context, we found five X-ray structures of ODC that should correspond to hypothetical snapshots of the reaction mechanism that we propose to study (Scheme 2 and Figure 2).

The PDB structure with the reference 2OO0 (human ODC) was crystallized in the presence of the potent inhibitor 1-(aminooxy)-3-aminopropane.[16] This structure contains PLP inside the active site pocket but not covalently bound to Lys69, which is involved in the formation of the internal aldimine.[16] This structure should resemble the reactants of the reaction that we wish to study, shortly after the PLP molecule binds the enzyme, but before the formation of the internal aldimine. Lys69 is pointing in the opposite direction of PLP and interacting very closely with the Asp88 carboxylate.[16] In such a conformation the enzyme is inactive.

Another interesting PDB structure is the mutated structure of ODC from *Trypanossoma brucei* (PDB 1SZR).[29] In this structure, Lys294 was mutated by an alanine. This residue is far away from the active site but has affected the nature of the ligand-bound species. Each of the four active sites contains unusual ligands, and two of them contain tetrahedral adducts involving PLP, Lys69, and a hydroxide (or even a water molecule).[29] These intermediates are very interesting as they resemble the carbinolamine intermediate that was proposed by Metzler,[30] which has absorption bands in the range of 325−335 nm,[31] but were not yet identified in studies with PLP enzymes. Moreover, the two 1SZR active sites with these tetrahedral adducts reveal two conformations for Cys360. The "on" position is found in active site 1SZR^{D}, and the "off" position is found in active site 1SZR^{C},[29] but also in PDB 1QU4.[32]

The PDB structure 1QU4, from the ODC of the same organism, also provides useful information.[32] All the active sites of the dimers have Lys69 bonded to PLP through a Schiff linkage. This structure corresponds to the final product, i.e., the internal aldimine. A similar structure is observed in the active site of the PDB structure 7ODC. Here, however, the active site lysine is slightly rotated, bringing N10 closer to O1 (see the atom numbering in Scheme 2). Since the most active form of the internal aldimine has a *cisoid* conformation,[1] this 7ODC structure might correspond to the most abundant conformation of the internal aldimine found in PLP-dependent enzymes.

All these structures were taken into consideration while studying the formation of the internal aldimine. In this process, several pathways were explored, but to simplify the discussion, only the most favorable ones will be presented. The overall reaction can be separated into three main steps that will be described in the following section, i.e., (i) the nucleophilic attack of the active site lysine to PLP, (ii) the carbinolamine formation, and (iii) the dehydration step.

3.1. Nucleophilic Attack of Lys69 on PLP. We started this study using the PDB structure 2OO0, which resembles the enzyme in the inactive form. In this structure, the PLP is already fitted inside the binding site but still unbonded from Lys69. The first reaction that we simulated was therefore the nucleophilic attack of N10 on C8 (Scheme 3).

In the optimized geometry of the reactants (Supporting Information, structure S1) N10 is 2.53 Å from C8 and is stabilized by two residues: Tyr389 (2.54 Å) and Cys360 (2.94 Å). Lys69 is placed right in front of C8 and in a perpendicular plane to the PLP ring (the angle of N10−C8−C7 is 93.1°), in this way favoring the reaction without any stereointerference. Atom C8 bears a slightly positive charge (0.72 au), which favors the

Scheme 3. First Step of the Mechanism Involving the Nucleophilic Attack of N10 on O1[a]

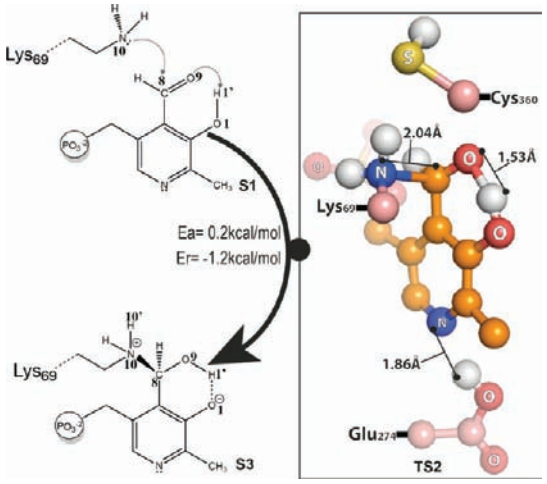

[a] The transition-state structure of this reaction is depicted in ball and stick format. The electronic energies were obtained by single-point calculations at the M06/6-311++G(2d,2p)//B3LYP/6-31G(d)) level.

nucleophilic attack. The large positive charge of C8 is attributed to the extended π conjugation in the PLP/pyridine ring system that makes it behave as an electron sink. Part of the electrophilic character of C8 is due to the intramolecular hydrogen bond between the hydroxyl and the aldehyde groups of the cofactor ($d_{O9:H1'}$ = 1.62 Å) that stabilizes the negative charge that develops at O9 and O1.

Subsequently, we optimized the structure in the scan with the highest energy to get the transition-state structure. Its nature was next verified by analyzing the vibrational frequencies. The highest imaginary frequency (101i cm^{-1}) coincides with a stretching of the atoms that are directly involved in the reaction—N10, C8, and also O9, H1′, and O1.

Transition state TS2 (Supporting Information) does not involve any significant geometric change when compared to the reactants except the closer contact between N10 and C8, which changed from 2.53 to 2.04 Å. The nucleophilic attack of the nitrogen atom N10 on the carbonyl C8 occurs through a characteristic angle that is a common feature in this type of reaction, as suggested by Bürgi and Dunitz.[33] As such, the angle N10−C8−O9 varies from 102.3° in the reactant structure S1 (Supporting Information) to 106.7° in the product structure S3 (Supporting Information).

In the product of this reaction (Supporting Information, structure S3), Lys69 becomes covalently bonded to C8 (1.58 Å). Consequently, C8 changes its hybridization from sp^2 to sp^3, and the positive charge now becomes concentrated at N10 (N10 changes from −0.40 au in structure S1 (Supporting Information) to 0.01 au in structure S3). In addition, the hydrogen H1 that was previously bound to O1 in the reactants now becomes connected to O9 (1.58 Å). This means that once Lys69 binds to PLP, the aldehyde from PLP is converted into a hydroxyl. These two functional groups continue to interact with each other through the same short intramolecular hydrogen bond (1.54 Å), but O1 starts to interact with Arg154 (2.03 Å). This effect seems to be important for the progression of the reaction.

The overall reaction has a very low activation barrier (0.2 kcal/mol), and it is almost thermoneutral (−1.2 kcal/mol). These results show that, once PLP binds to the active site, the nucleophilic attack

Scheme 4. Schematic Representation of Some of the Pathways That Were Explored Leading to the Formation of the Carbinolamine Intermediate[a]

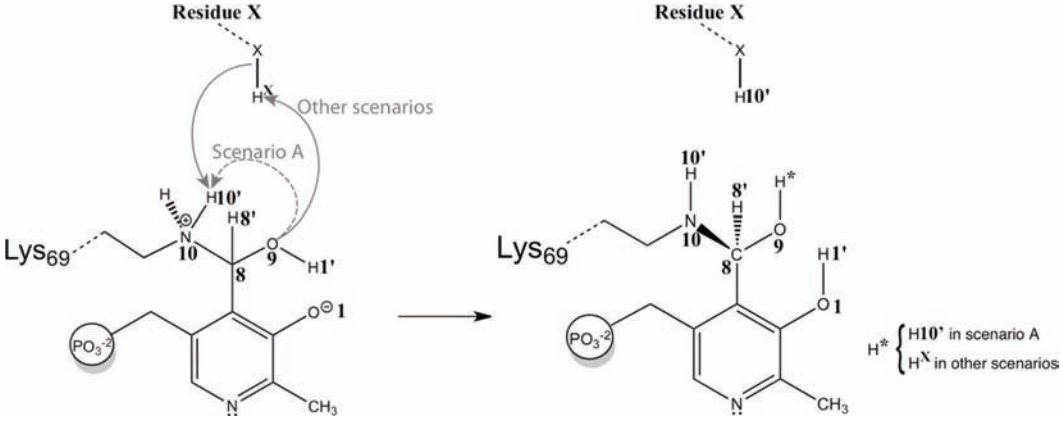

[a] Scenario A: direct proton transfer from N10 to O9. Scenarios B−D: reactions in which Tyr360, Cys360, or water mediates the proton transfer between N10 and O9.

of Lys69 is almost spontaneous, but it can be easily reverted. During this process neither the PLP nor the active site undergoes significant conformational rearrangements, which ensures an easy interchange between both states.

3.2. Formation of the Carbinolamine Intermediate. According to the proposal made by Metzler et al., the next step should involve the formation of a carbinolamine intermediate.[30] This reaction requires a proton transfer from N10 to PLP (O1 or O9) (Scheme 4). The final product of this reaction should be very similar to the ligand that was crystallized by Jackson et al. in the mutated ODC (PDB entry 1SZR).[29]

Multiple pathways can be drawn for this step, as depicted in Scheme 4. Scenario A involves the direct proton transfer from N10 to O9. Scenarios B and C in the same scheme involve the participation of a neighboring proton donor/acceptor residue (residue X in Scheme 4) capable of mediating the proton transfer. Two residues are positioned to play such a role, namely, Cys360 and Tyr389 (Scheme 1). Cys360 has the thiol sulfur 3.9 and 4.5 Å from O9 in the PDB structures 2OO0 and 1SZR. In the PDB structure 1SZR, Cys360 sulfur is 3.0 Å from N10. Tyr389 is not so close to this center, but the flexibility of the side chain may allow it to interact with atoms N10 and O9 (3.2 and 4.0 Å in the 2OO0 structure and 4.3 and 4.4 Å in the 1SZR structure).

Another possibility is the involvement of a water molecule in the course of this reaction (scenario D), similar to what was proposed by several authors.[9] Looking at the PDB structures that were analyzed before (Figure 2), only two (7ODC and 1SZR) have a water molecule in an appropriate position to mediate this reaction. However, the 7ODC structure should be excluded from this analysis because it already has the internal aldimine formed in the active site and, as will be seen later, the formation of such a compound requires the formation and release of one water molecule. This means that the water molecule seen in the X-ray structure is probably a product of the reaction and may not be available beforehand to mediate the proton transfer. The other structure (1SZR) contains an intermediate that resembles the product of this reaction (the carbinolamine) and a water molecule (Wat631) that is located in a suitable position to mediate the proton transfer. However, many authors believe that the presence of this water molecule is an artifact that is caused by the extensive disorder of the active site promoted by the mutated protein.[29,34] This means that the presence of a water molecule in the active site region at this stage of the reaction is very unlikely. Even though other studies have included a water molecule to mediate this proton transfer,[9] we have also modeled this reaction and compared the results with the other pathways and previous suggestions.

All of these scenarios were carefully and individually explored, and some of them turned out to be more favorable than others. The direct proton transfer from scenario A and the proton transfer mediated by Tyr389 (scenario B) were soon discarded due to the high activation barriers that they require (E_a = 42.3 and 40.3 kcal/mol) (Figure 3). The main reasons behind this behavior are several. In the direct proton transfer (scenario A), the long distance between the N10 proton and its acceptor ($d_{O9:H10'}$ = 4.1 Å) and the steric hindrance that arises from the proximity of atoms N10 and O9 at the transition state were determinants for the prohibitive activation barrier. Concerning the proton transfer mediated by Tyr389 (scenario B), the restricted mobility of this residue was the main cause that precluded the feasibility of this reaction. The other two scenarios (C and D) in which a water molecule or Cys360 participates in the proton transfer were kinetically and thermodynamically more favorable. In both scenarios, the optimized structures of the reactants are very similar. N10 remains covalently bound to C8 (1.58 Å). Atoms O9 and O1 continue to interact very closely via a hydrogen bond. The nitrogen of the pyridine ring remains unprotonated and interacts very closely with Glu274 by a hydrogen bond (~1.75 Å). In both scenarios Cys360 (scenario C) and the water molecule (scenario D) are placed between N10 and O9 ($d_{N10:S}$ = 3.45 Å and $d_{O9:S}$ = 3.17 Å in scenario C and $d_{N10:OW}$ = 2.73 Å and $d_{O9:OW}$ = 2.76 Å in scenario D), foreseeing two coupled proton transfers. In spite of these similarities, the mechanism by which the carbinolamine intermediate was obtained differs in both cases. When the water molecule participates in the reaction, the carbinolamine is obtained in a single step, while the involvement of Cys360 requires two steps.

The direct participation of the water molecule in the formation of the carbinolamine intermediate requires an activation energy of 19.9 kcal/mol and is very exergonic (−27 kcal/mol) (Scheme 5). The reaction occurs in a single step and involves

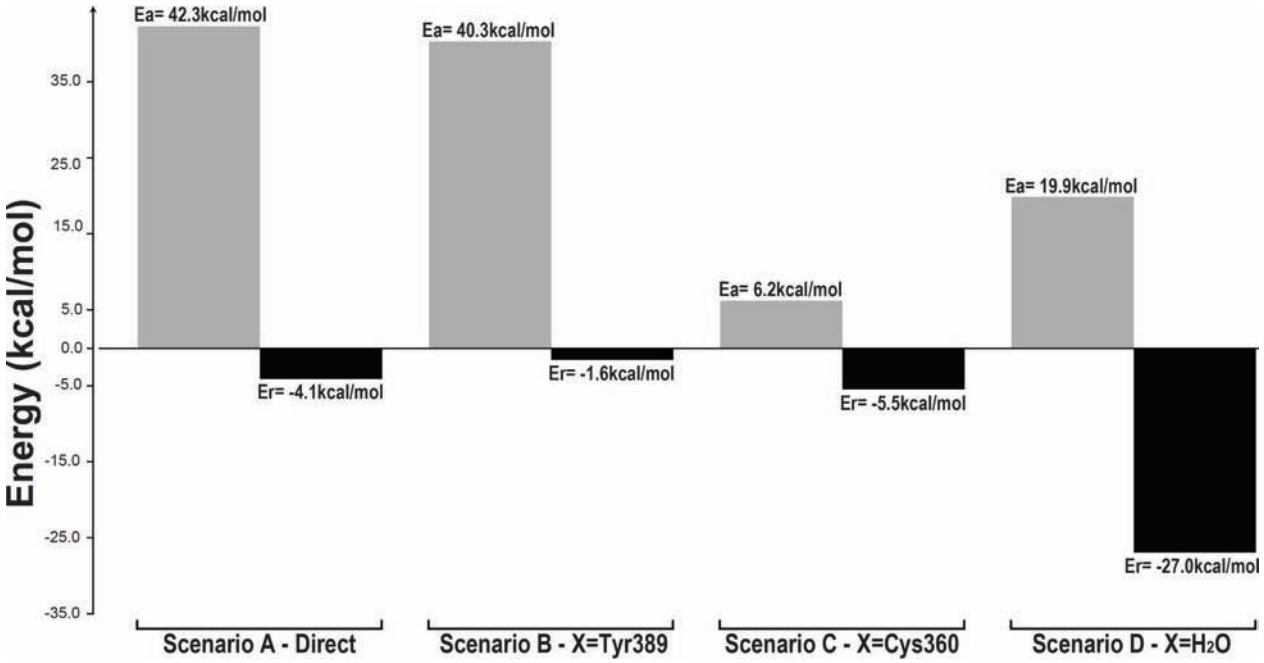

Figure 3. Energies involved in the four scenarios used to study the formation of the carbinolamine intermediate. Scenario 1: direct proton transfer between Lys69 and O9. Scenarios 2−4: reactions in which Tyr360, Cys360, and water mediate the proton transfer between N10 and O9 (activation energies are colored in gray and the reaction energies in black). The electronic energies were obtained by single-point calculations at the M06/6-311++G(2d,2p)//B3LYP/6-31G(d)) level.

Scheme 5. Second Step of the Formation of the Carbinolamine Intermediate Mediated by a Water Molecule[a]

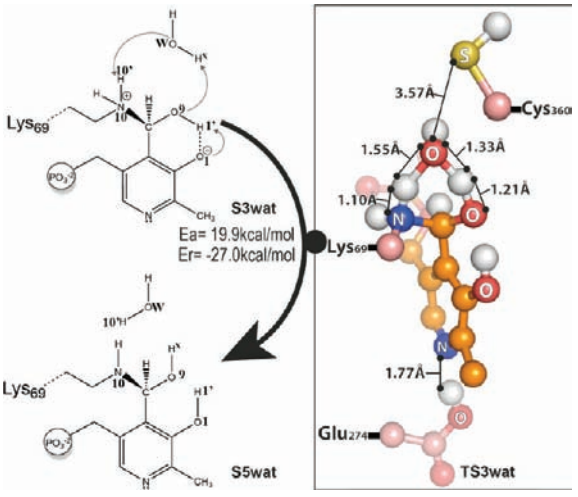

[a] The transition-state structures of this reaction are depicted in ball and stick format. The electronic energies were obtained by single-point calculations at the M06/6-311++G(2d,2p)//B3LYP/6-31G(d)) level.

three coupled proton transfers; i.e., at the same time that one proton (H10′) migrates from N10 to water atom OW, one proton from the latter is abstracted by O9 and the proton bonded to O9 (H1′) is transferred back to O1, originating the carbinolamine intermediate. At transition state TS3wat (Supporting Information), the water molecule is very close to PLP ($\mathbf{d}_{OW:C8}$ = 2.90 Å) and the three protons are already halfway between the nucleophilic atoms and the proton donors. The structure that is obtained in the end of this reaction (S4wat, Supporting Information) is very similar to the reactants but with the following differences: (i) O1 is now protonated and (ii) the hybridization state of N10 changes from sp^3 to sp^2.

When Cys360 participates in the reaction, the carbinolamine moiety is only obtained after two sequential steps (Scheme 6). The first step involves two concerted proton transfers: (i) the proton transfer between the sulfur atom of Cys360 and O9 and (ii) the proton transfer from atom O9 to O1. At transition state TS4 (Supporting Information), both protons are halfway between the nucleophilic atoms and the proton donors and Cys360 becomes negatively charged (−0.52 au). At the end of this reaction (structure S5, Supporting Information), two hydroxyl groups are found in PLP at C8 and C1 and Cys360 remains negatively charged (−0.69 au). This reaction requires a low activation energy (6.2 kcal/mol), and it is endergonic (1.3 kcal/mol). The second step of this reaction involves the abstraction of one proton from N10 by the thiolate of Cys360. The closest hydrogen atom from this center is H10′, and it is 2.04 Å away from the thiolate sulfur. At transition-state structure TS6 (Supporting Information), proton H10′ is midway between N10 and the sulfur atom of Cys360 ($d_{N10:H10'}$ = 1.34 Å; $d_{S:H10'}$ = 1.68 Å). In the product of this reaction (structure S7, Supporting Information), the carbinolamine intermediate is obtained and Cys360 becomes protonated. Structure S7 is very similar to the one that was obtained before, when the water molecule was used to catalyze a similar reaction (S3wat). The activation energy of this reaction is 1.0 kcal/mol, and the reaction is slightly exergonic (−6.8 kcal/mol). The overall energetic profile when Cys360 is used in the proton transfer is very favorable, requiring very low activation barriers (6.2 kcal/mol), and it is slightly exergonic (−5.5 kcal/mol).

Comparing the results obtained with the water molecule (scenario D) and with Cys360 (scenario C), we can see that the latter is more favorable. This result reinforces the idea that a water molecule is not required to mediate the proton transfer.

Scheme 6. Second Step of the Mechanism Involving the Formation of the Carbinolamine Intermediate, Mediated by Cys360[a]

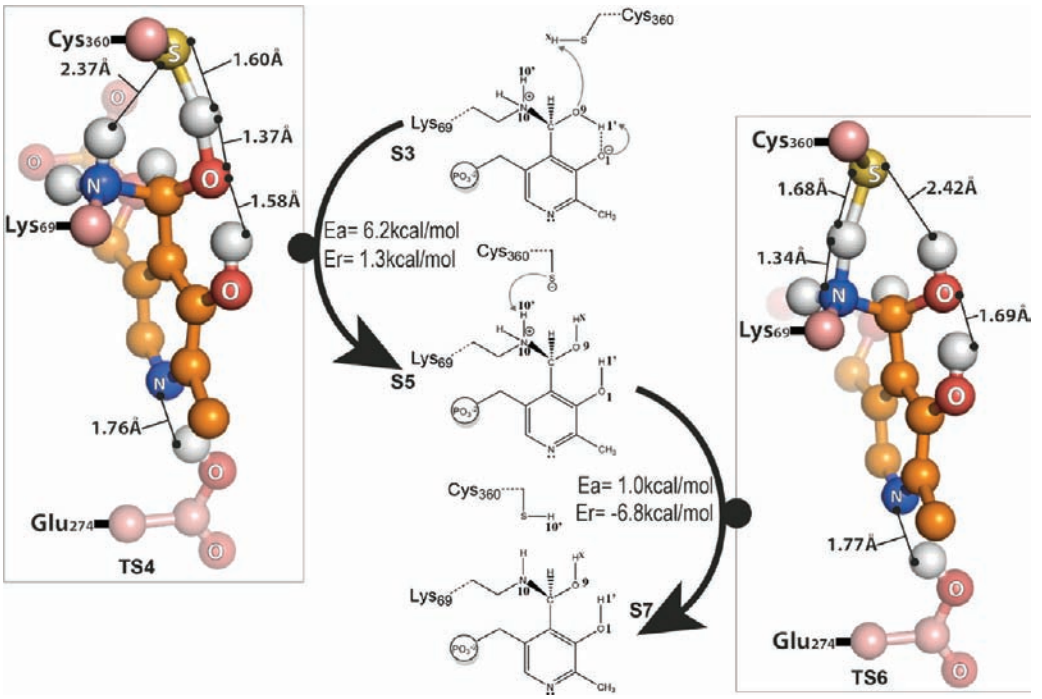

[a] The transition-state structure of this reaction is depicted in ball and stick format. The electronic energies were obtained by single-point calculations at the M06/6-311++G(2d,2p)//B3LYP/6-31G(d)) level.

In fact, there are several pieces of experimental evidence that support the involvement of Cys360 in this step. Several X-ray structures show that Cys360 can adopt two conformations during the formation of the carbinolmine intermediate which were previously referred as the "on" and "off" conformations.[29] The on conformation can be found in PDB structure 1QUA and corrresponds to a rotamer of Cys360 pointing toward PLP. This corresponds to the conformation prior to the formation of the carbinolamine intermediate. The off conformation can be found in PDB structure 7ODC, with Cys more distant from PLP and pointing toward the opposite direction. This pattern is also becoming apparent in the products of scenario C in which Cys360 is moving away from the PLP ($d_{S:C8}$ = 3.57 Å in structure S3 (Supporting Information) changes to 3.91 Å in structure S7 (Supporting Information)).

A mechanistic role for the conserved Cys360 in the course of the reaction was already suspected. For instance, in ODC it was suggested that Cys360 should have an active role during the decarboxylation step, where it could act as a general acid or help the decarboxylation through the orientation of the carboxylate group of the substrate.[29,32,35] A previous work from Jackson et al. showed that the mutation of Cys360 to an alanine decreased the k_{cat} of the enzyme by 50-fold.[36−38] As the decarboxylation step became the rate-limiting step of the studied reaction, the authors proposed that Cys360 might be important for decarboxylation. Our work gives new insights to interpret these results: besides a possible role of Cys360 during decarboxylation, we show that Cys360 has an active and important role in the formation of the internal aldimine. The activity of Cys360-mutated proteins can be explained if we consider that a water molecule can substitute the mechanistic role of Cys360. Our results suggest that the reaction can also be catalyzed by a water molecule, albeit not so efficiently.

Scheme 7. Third Step of the Mechanism from Which Results the Internal Aldimine and the Formation of One Water Molecule[a]

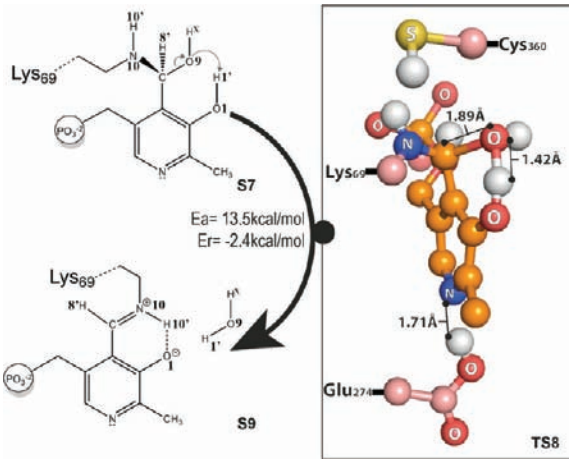

[a] The transition-state structure of this reaction is depicted in ball and stick format. The electronic energies were obtained by single-point calculations at the M06/6-311++G(2d,2p)//B3LYP/6-31G(d)) level.

3.3. Dehydration of the Carbinolamine. To generate the internal aldimine, the carbinolamine intermediate structure S7 (Supporting Information) has to be dehydrated. Therefore, a proton must be transferred from O1 to O9, leading to the breaking of the C7−O9 bond. In the end of the reaction a water molecule is obtained (Scheme 7).

In the reactants, both hydroxyl groups are bonded to PLP ($d_{C2:O1}$ = 1.37 Å and $d_{C8:O9}$ = 1.49 Å), and they interact very

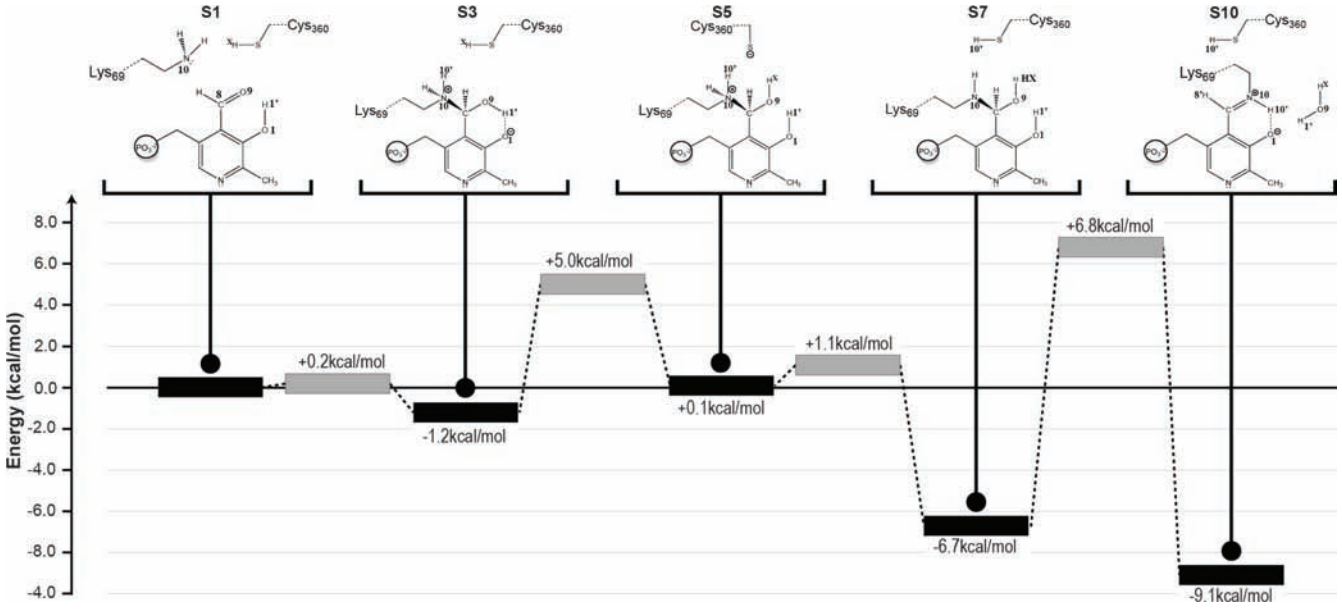

Figure 4. Most favorable pathway for the formation of the internal aldimine. The electronic energies were obtained by single-point calculations at the M06/6-311++G(2d,2p)//B3LYP/6-31G(d)) level.

closely with each other through a short intramolecular hydrogen bond (1.69 Å between heavy atoms).

At the transition state of this reaction (TS8, Supporting Information), the formation of the water molecule is almost accomplished. The C8−O9 bond length increases to 1.89 Å. At the same time the C8−N9 bond length decreases to 1.34 Å (1.41 Å in the reactants). In this structure, hydrogen H1′ becomes closer to atom O9 (1.42 Å vs 1.69 Å in the reactants) but it remains bonded to O1 (1.07 Å vs 1.00 Å in the reactants).

In the products the water molecule disconnects from PLP($d_{O9\cdot C8}$ = 4.95 Å). It becomes stabilized in the active site region through hydrogen bonds with the side chains of Arg154 and Cys360 and with O1 (2.03, 2.19, and 1.83 Å). Cys360, previously close to PLP (S−C8 distance of 3.91 Å in the products of the previous step), rotates and points toward the opposite direction (S−C8 distance of 5.14 Å). This corresponds to the off conformation of Cys360 that was discussed in the preceding section and resembles what is found in the PDB structures 1SZR[C] and 1QU4 (Figure 2). This conformational rearrangement enables Lys69 to become coplanar with PLP, in such a way that proton H10′ makes a hydrogen bond with O1 (1.75 Å). In the end of this reaction a very stable zwitterionic structure is obtained (structure S9, Supporting Information), with a C8−N10 bond length of 1.30 Å. This *cisoid* structure with a double bond aldimine and O1 deprotonated (with a bond order between simple and double) coincides with the most active form of piridoxaldimine found in PLP-dependent enzymes.[1] In the full course of this reaction nitrogen N4 remained unprotonated.

This reaction requires an activation energy of 13.5 kcal/mol and is exergonic (−2.4 kcal/mol). The PLP complex that was obtained in the end of this reaction is very similar to the one that can be found in the X-ray structure 7ODC, as is illustrated by Figure 2. All the bond lengths are very similar, and the water molecule occupies similar positions in the binding site.

4. CONCLUSIONS

In this investigation we have studied the formation of the internal aldimine, a common step in the activation of the majority of the PLP-dependent enzymes. This process involves the nucleophilic attack of an active site lysine (Lys69) on PLP with the formation of a Schiff base. The formation of such a complex is very important since it commands the activity of these enzymes. In addition, it is essential to shape the PLP orientation inside the active site, a condition that controls and determines the type of reaction catalyzed by each PLP-dependent enzyme, in the subsequent reactions.

Earlier calculations, based on small cluster models, have proposed catalytic pathways that clarified important aspects of the formation of the internal aldimine. However, several experimental results cannot be fitted in those proposals, and most of them lack the presence/participation of the enzyme in the full process. The present results provide for the first time a complete mechanistic portrait of the formation of the internal aldimine in an enzymatic environment that is fully consistent with all available experimental data.

The results obtained in this work show that the full process is accomplished in three sequential steps, in which Cys360 plays a key role. The overall reaction is exergonic (−9.1 kcal/mol). The rate-limiting step of the full process is the dehydration step, with an activation energy of 13.5 kcal/mol. The full mechanism of this reaction is depicted in Figure 4.

Briefly, the first step of this mechanism involves the nucleophilic attack of Lys69 on PLP. In this process, Lys69 must be in a preactive conformation, in such a way that it becomes aligned with the PLP ring. This step is almost spontaneous and does not require the presence of an auxiliary water molecule. In the second step, several possibilities were evaluated, but one turned out to be the most favorable. It involves the direct participation of Cys360 in the formation of the carbinolamine intermediate that is experimentally detected. This reaction has a very low energetic profile and requires two sequential proton transfers: (i) from Lys69 to Cys360 and (ii) from Cys360 to one hydroxyl group of PLP. Once this intermediate is obtained, the formation of the internal aldimine is straightforward, involving only the formation of one water molecule that becomes trapped inside the active site,

similarly to what is observed in the PDB structure 7ODC. This is accomplished with a proton transfer from atom O1 to O9 and the concomitant bond cleavage between atoms C8 and O9. This process is the rate-limiting step of the full reaction requiring an activation energy of 13.5 kcal/mol.

The results obtained in this study show for the first time the importance of Cys360 as an active residue in the formation of the internal aldimine. Our studies have also shown that even when a water molecule is placed in a favorable way inside the active site, this reaction is less favorable than the one mediated by Cys360. We also tried to model other possibilities, for instance, the direct proton transfer between Lys69 and the PLP molecule or even the participation of Tyr359 to mediate the proton transfer, but all of them turn out to be very unfavorable when compared to the one that involves Cys360.

The involvement of Cys360 in the mechanism is also well supported by several experimental data. Indeed, several X-ray structures containing some intermediates of this reaction show that Cys360 can be found in two different conformations that are visible in the reaction that was modeled in this study, i.e., the on and the off conformations. Furthermore, the intermediates obtained in the course of the model reaction are very similar to the compounds that are found in many PDB structures such as 2OO0, 1SZR, and 7ODC, giving us confidence about the reproducibility of this reaction in vivo. Taking into account that the active site of most PLP-dependent enzymes is very conserved, particularly the active site lysine and cysteine, we believe that the mechanism presented here should be general for most of PLP-dependent enzymes.

■ ASSOCIATED CONTENT

Supporting Information. Absolute energies and coordinates of the atoms of all optimized structures. This material is available free of charge via the Internet at http://pubs.acs.org.

■ AUTHOR INFORMATION

Corresponding Author
mjramos@fc.up.pt

■ ACKNOWLEDGMENT

This work has been financed by the program FEDER/COMPETE and by the Fundação para a Ciência e a Tecnologia (Project PTDC/QUI-QUI/102760/2008).

■ REFERENCES

(1) Jansonius, J. N. *Curr. Opin. Struct. Biol.* **1998**, *8*, 759.
(2) Eliot, A. C.; Kirsch, J. F. *Annu. Rev. Biochem.* **2004**, *73*, 383.
(3) Braunstein, A.; Shemyakin, M. *Biokhimiya* **1953**, *18* (393), 411.
(4) Metzler, D. E.; Ikawa, M.; Snell, E. E. *J. Am. Chem. Soc.* **1954**, *76*, 648.
(5) Sayer, J.; Conlon, P. *J. Am. Chem. Soc.* **1980**, *102*, 3592.
(6) Hershey, S. A.; Leussing, D. L. *J. Am. Chem. Soc.* **1977**, *99*, 1992.
(7) Sayer, J.; Pinsky, B.; Schonbrunn, A.; Washtien, W. *J. Am. Chem. Soc.* **1974**, *96*, 7998.
(8) Sayer, J.; Jencks, W. *J. Am. Chem. Soc.* **1977**, *99*, 464.
(9) Salvà, A.; Donoso, J.; Frau, J.; Muñoz, F. *J. Phys. Chem. A* **2003**, *107*, 9409.
(10) Sonnet, P. E.; Mascavage, L. M.; Dalton, D. R. *Bioorg. Med. Chem. Lett.* **2008**, *18*, 744.
(11) Himo, F. *Theor. Chem. Acc.* **2006**, *116*, 232.
(12) Leopoldini, M.; Marino, T.; Michelini, M. D.; Rivalta, I.; Russo, N.; Sicilia, E.; Toscano, M. *Theor. Chem. Acc.* **2007**, *117*, 765.
(13) Ramos, M. J.; Fernandes, P. A. *Acc. Chem. Res.* **2008**, *41*, 689.
(14) Alberto, M. E.; Marino, T.; Ramos, M. J.; Russo, N. *J. Chem. Theory Comput.* **2010**, *6*, 2424.
(15) Cerqueira, N. M. F. S. A.; Fernandes, P. A.; Ramos, M. J. *Chem.—Eur. J.* **2007**, *13*, 8507.
(16) Dufe, V.; Ingner, D.; Heby, O.; Khomutov, A.; Persson, L.; Al-Karadaghi, S. *Biochem. J.* **2007**, *405*, 261.
(17) *Accelrys Discovery Studio*; Accelrys: San Diego, CA, 2007.
(18) Dapprich, S.; Kom·romi, I. n.; Byun, K. S.; Morokuma, K.; Frisch, M. J. *J. Mol. Struct.: THEOCHEM* **1999**, *461−462*, 1.
(19) Vreven, T.; Morokuma, K. *J. Comput. Chem.* **2000**, *21*, 1419.
(20) Cerqueira, N. M. F. S. A.; Fernandes, P. A.; Eriksson, L. A.; Ramos, M. J. *J. Comput. Chem.* **2004**, *25*, 2031.
(21) Frisch, M. J.; et al. *Gaussian 09*, revision A.1; Gaussian, Inc.: Wallingford, CT, 2009.
(22) Cerqueira, N. M. F. S. A.; Fernandes, P. A.; Ramos, M. J. *J. Chem. Theory Comput.* **2011**, *7*, 1356.
(23) Dewar, M. J. S.; Zoebisch, E. G.; Healy, E. F.; Stewart, J. J. P. *J. Am. Chem. Soc.* **1985**, *107*, 3902.
(24) Mackie, I. D.; DiLabio, G. A. *J. Phys. Chem. A* **2008**, *112*, 10968.
(25) Zhao, Y.; Truhlar, D. G. *Acc. Chem. Res.* **2008**, *41*, 157.
(26) Sousa, S. F.; Fernandes, P. A.; Ramos, M. J. *J. Phys. Chem. A* **2007**, *111*, 10439.
(27) Singh, U. C.; Kollman, P. A. *J. Comput. Chem.* **1984**, *5*, 129.
(28) Besler, B. H.; Merz, K. M.; Kollman, P. A. *J. Comput. Chem.* **1990**, *11*, 431.
(29) Jackson, L. K.; Baldwin, J.; Akella, R.; Goldsmith, E. J.; Phillips, M. A. *Biochemistry* **2004**, *43*, 12990.
(30) Christen, P.; Metzler, D. E. *Transaminases*; John Wiley & Sons: New York, 1985.
(31) Sevilla, J. M.; Blazquez, M.; Dominguez, M.; Garciablanco, F. *J. Chem. Soc., Perkin Trans. 2* **1992**, 921.
(32) Grishin, N.; Osterman, A.; Brooks, H.; Phillips, M.; Goldsmith, E. *Biochemistry* **1999**, 38.
(33) Burgi, H. B.; Dunitz, J. D.; Lehn, J. M.; Wipff, G. *Tetrahedron* **1974**, *30*, 1563.
(34) Myers, D. P.; Jackson, L. K.; Ipe, V. G.; Murphy, G. E.; Phillips, M. A. *Biochemistry* **2001**, *40*, 13230.
(35) Swanson, T.; Brooks, H. B.; Osterman, A. L.; O'Leary, M. H.; Phillips, M. A. *Biochemistry* **1998**, *37*, 14943.
(36) Jackson, L. K.; Brooks, H. B.; Osterman, A. L.; Goldsmith, E. J.; Phillips, M. A. *Biochemistry* **2000**, *39*, 11247.
(37) Osterman, A.; Grishin, N. V.; Kinch, L. N.; Phillips, M. A. *Biochemistry* **1994**, *33*, 13662.
(38) Coleman, C. S.; Stanley, B. A.; Pegg, A. E. *J. Biol. Chem.* **1993**, *268*, 24572.